JOC The Journal of Organic Chemistry

pubs.acs.org/joc Article

Rules for Magnetic Exchange in Azulene-Bridged Biradicals: *Quo Vadis*?

Patrick Hewitt, David A. Shultz,* and Martin L. Kirk*

Cite This: https://doi.org/10.1021/acs.joc.1c02085 Read Online

ACCESS | Metrics & More | Article Recommendations | Supporting Information

ABSTRACT: Electronic coupling through organic bridges facilitates magnetic exchange interactions and controls electron transfer and single-molecule device electron transport. Electronic coupling through alternant π-systems (*e.g.*, benzene) is better understood than the corresponding coupling through nonalternant π-systems (*e.g.*, azulene). Herein, we examine the structure, spectroscopy, and magnetic exchange coupling in two biradicals (**1,3-SQ$_2$Az** and **1,3-SQ-Az-NN**; SQ = the zinc(II) complex of spin-1/2 semiquinone radical anion, NN = spin-1/2 nitronylnitroxide; Az = azulene) that possess nonalternant azulene π-system bridges. The SQ radical spin density in both molecules is delocalized into the Az π-system, while the NN spin is effectively localized onto the five-atom ONCNO π-system of NN radical. The spin distributions and interactions are probed by EPR spectroscopy and magnetic susceptibility measurements. We find that J = +38 cm^{-1} for **1,3-SQ$_2$Az** and J = +9 cm^{-1} for **1,3-SQ-Az-NN** ($\mathcal{H} = -2J\hat{S}_{SQ}\cdot\hat{S}_{SQorNN}$). Our results highlight the differences in exchange coupling mediated by azulene compared to exchange coupling mediated by alternant π-systems.

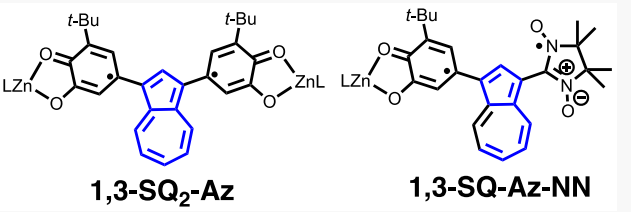

INTRODUCTION

Molecular electronic coupling figures prominently in electron transfer rates and electron transport efficiency involving molecular bridges (B) that span donor and acceptor units in molecules (D-B-A) and in biased electrodes/molecular break junctions (M-B-M), respectively. Electronic coupling has been suggested to be a transferable property of the molecular bridge,[1,2] enabling further relationships between electron transfer/transport and the bridge-dependent magnetic superexchange interaction to be developed. Understanding the nature of electronic and magnetic communication will enhance our ability to design bespoke electronic, spintronic, and related molecular or molecule-based devices.[3−13] Electronic coupling through alternant organic π-systems (*e.g.*, benzene) has been studied extensively and can be illustrated by topographical models and concepts such as resonance,[14] aromaticity,[15−17] and cross-conjugation.[15,18−22] Recently, this has been exploited to relate the magnetic exchange interaction with molecular conductance and rectification mediated by alternant and alternant-like organic π-systems.[2,23] In spite of our knowledge of electronic and magnetic coupling in alternant systems, the corresponding coupling through nonalternant π bridges[24] is markedly less understood.[25,26] This is exemplified by the fact that computationally aided analysis of, and transport through, the nonalternant π-system of azulene has produced both debate and seemingly conflicting experimental results.[27−29] As a quintessential nonalternant π-system, azulene has been of interest for nearly five decades for its unique photophysical, optical, and electronic properties and has gained renewed interest as a key molecule in organic electronics.[27,30−38] Despite their technological importance, there is a paucity of studies directed toward understanding the nature of the electronic and magnetic coupling mediated by azulenes and related nonalternant systems.[25,26,39−41] A rare example of magnetic communication through a nonalternant π-system was recently described by Haraguchi *et al.*,[42] who reported differential magnetic exchange coupling of iminonitroxides (IN) and nitronylnitroxides (NN) covalently attached to the 1,3-positions of azulene (**1,3-IN$_2$Az** and **1,3-NN$_2$-Az**, Figure 1).

Magnetic-exchange interactions mediated by organic bridges have been a subject of intense theoretical and experimental research, and the electronic origin of both the sign and magnitude of the exchange interaction is typically cast in terms of the active-electron approximation.[45,46] Borden and Davidson classified biradicals as either nondisjoint or disjoint (Figure 2A,B, respectively),[47] and within this active-electron approximation nondisjoint biradicals possess substantial singly occupied molecular orbital (SOMO) overlap densities and consequently have large exchange integrals. Thus, they are predicted to exhibit ferromagnetic exchange via Hund's first rule.[48−51] In marked contrast, disjoint biradicals have no SOMO

Received: August 27, 2021

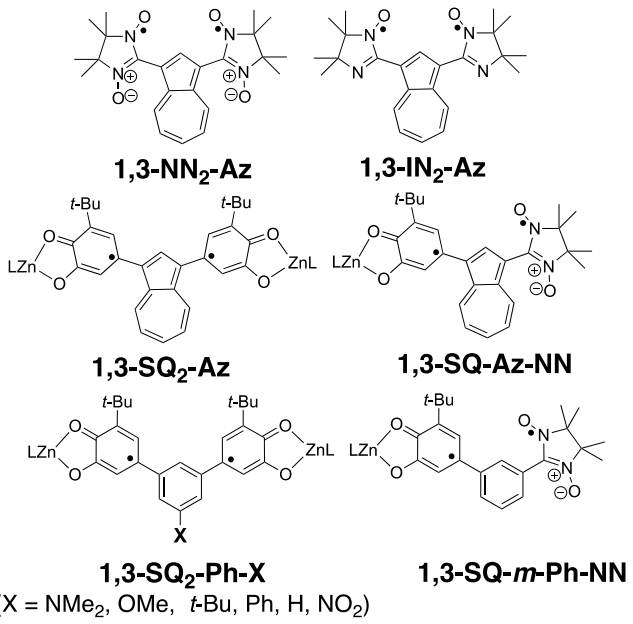

Figure 1. Biradicals and metal complexes of biradical ligands with nonalternant π-system bridges: **1,3-IN$_2$Az** and **1,3-NN$_2$Az** (top), **1,3-SQ$_2$Az** and **1,3-SQ-Az-NN** (middle), and alternant π-system bridges **1,3-SQ$_2$Ph-X**[43,44] and **1,3-SQ-*m*-Ph-NN** (bottom).

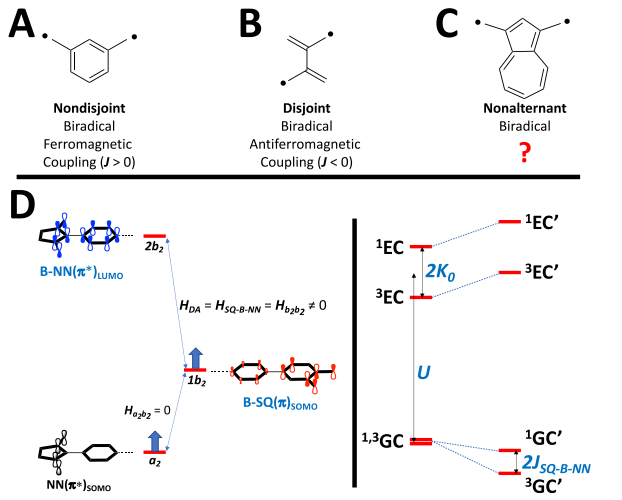

Figure 2. Nondisjoint (A), disjoint (B), and nonalternant (C) biradicals. (D) SQ-B-NN donor–acceptor biradical VBCI Model. The a_2 and $1b_2$ orbitals are the NN and SQ SOMOs, respectively, and the $2b_2$ acceptor orbital is the NN LUMO. Singlet and triplet ground configurations (GCs) are $a_2^1 1b_2^1 2b_2^0$. Low-energy excited, singlet and triplet $a_2^1 1b_2^0 2b_2^1$ charge-transfer configurations (CTCs) mix into the GCs via $H_{SQ\text{-}NN} = H_{DA}$ to generate the ground singlet–triplet gap = $2J_{SQ\text{-}NN}$, which is determined as a fit parameter of variable-temperature magnetic susceptibility plots.

overlap density and therefore possess negligible exchange integrals. These systems are therefore predicted to exhibit either (typically weak) antiferromagnetic exchange interactions but display interesting physical properties and complex spin physics.[52,53] Notably, disjoint and nondisjoint alternant π-system biradicals can be understood in the context of Ovchinnikov's and Longuett-Higgins' "star/non-star"[54−56] formalism in addition to spin-polarization[50,57−60] methods. This design strategy has led to the synthesis of a multitude of high-spin organic molecules, dendrimers, and polymers.[61−75]

However, neither the active-electron approach *nor* the "star/non-star" method can account for the nature of the exchange coupling in biradicals bridged by nonalternant π-systems (*e.g.*, Figure 2C as well as **1,3-IN$_2$Az** and **1,3-NN$_2$-Az**). Furthermore, there are few examples of such biradicals. In this context, the results of Haraguchi *et al.* are notable since both **1,3-IN$_2$Az** and **1,3-NN$_2$-Az** are disjoint, yet **1,3-IN$_2$Az** exhibits weak antiferromagnetic coupling ($J = -3.0$ cm^{-1}) while **1,3-NN$_2$-Az** exhibits ferromagnetic coupling ($J = +6.9$ cm^{-1}).[42] Interestingly, these two disjoint biradicals lack both spin delocalization into the bridging unit and superexchange pathways that clearly related spectroscopic features.[76] This is not to say that there is no bridge spin density in NN-substituted azulenes, indeed there is.[42] However, since the NN SOMO is nodal at carbon, azulene spin density is derived from spin polarization rather than direct overlap of SOMO and bridge wave functions As a result, more structural types are required to elucidate the mechanisms that control magnetic- and electronic coupling through nonalternant π-system bridges.[77,78]

As an alternative to the active-electron approach, we have shown that magnetic exchange coupling in both nondisjoint,[47,79] and disjoint[76] donor-bridge-acceptor (D-B-A) biradicals can be treated using a spectroscopy-oriented valence bond configuration interaction (VBCI) approach, *e.g.*, Figure 2D. Our D-B-A triads are comprised of spin-1/2 3-*tert*-butyl-orthosemiquinone (SQ) donors and spin-1/2 NN acceptors. The advantage of using a VBCI/superexchange model is that spectroscopic and magnetic observables can be used to correlate $J_{SQ\text{-}B\text{-}NN}$ (determined by fitting variable-temperature magnetic susceptibility data) with the electronic coupling matrix element, $H_{D\text{-}B\text{-}A}$, in order to determine the excited-state origins of bridge-dependent electronic coupling, $H_{D\text{-}B\text{-}A}$.[80−82] This model is presented in Figure 2D, where $H_{SQ\text{-}B\text{-}NN} \equiv H_{D\text{-}B\text{-}A}$, K is the SQ → B-NN charge transfer (CT) excited state singlet–triplet gap, and U is the mean CT energy. We have recently used this idea to correlate superexchange pathways that give rise to magnetic exchange interaction with molecular electron transport pathways.[80,83−85]

To further explore magnetic exchange coupling mediated by nonalternant π-system bridges, we describe the synthesis and the nature of the magnetic exchange coupling in **1,3-SQ$_2$Az** and the D-B-A biradical, **1,3-SQ-Az-NN** (Figure 1). Unlike **1,3-IN$_2$Az** and **1,3-NN$_2$Az**, these new biradical complexes possess SQ donor groups that facilitate the delocalization of spin density directly onto the Az bridge fragment. We compare these new biradicals to **1,3-IN$_2$Az**, **1,3-NN$_2$Az**,[42] **1,3-SQ$_2$Ph**,[44] and **1,3-SQ-Ph-NN**,[76] and the results generated provide new insight into magnetic and electronic coupling mediated by both alternant and nonalternant organic π-systems. This work also addresses the important concept of "bridge transferability" between disparate D–B–A molecules and their corresponding molecular device constructs.[86]

RESULTS AND DISCUSSION

Synthesis. Biradical ligand metal complex **1,3-SQ$_2$Az** was synthesized as shown in Scheme 1. The synthesis begins with the bromination of azulene at both the 1- and 3-positions with *N*-bromosuccinimide in accordance with literature procedure.[37] 1,3-Dibromoazulene was subjected to Suzuki coupling with **MOM$_2$CatBpin** to give **1,3-(MOM$_2$Cat)$_2$Az**. The methoxymethyl (MOM) protecting groups were removed using catalytic HCl in MeOH at room temperature, and the resulting bis(catechol), **1,3-Cat$_2$Az** was complexed with Tp^{Cum,Me}Zn-

https://doi.org/10.1021/acs.joc.1c02085
J. Org. Chem. XXXX, XXX, XXX−XXX

Scheme 1. Synthesis of 1,3-SQ$_2$Az and 1,3-SQ-Az-NN

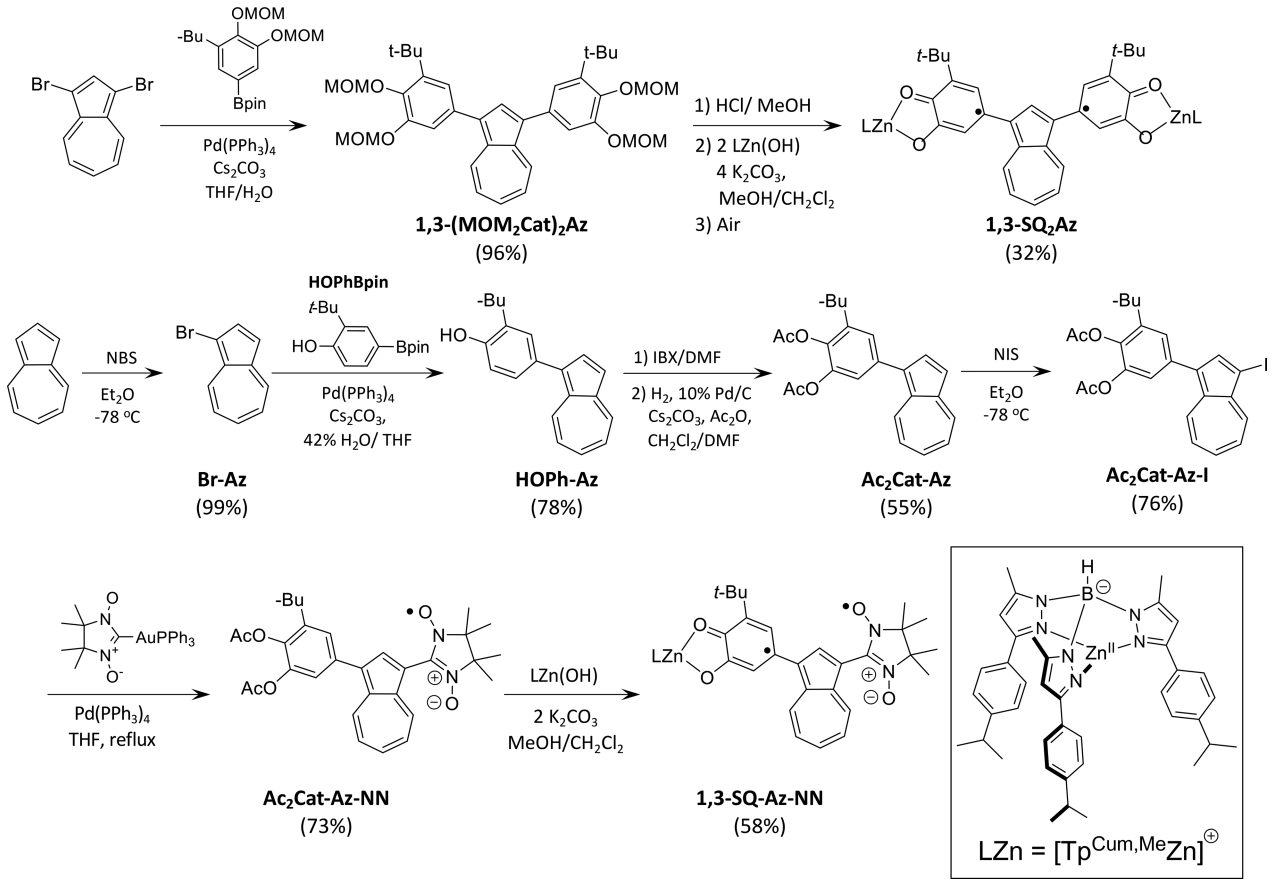

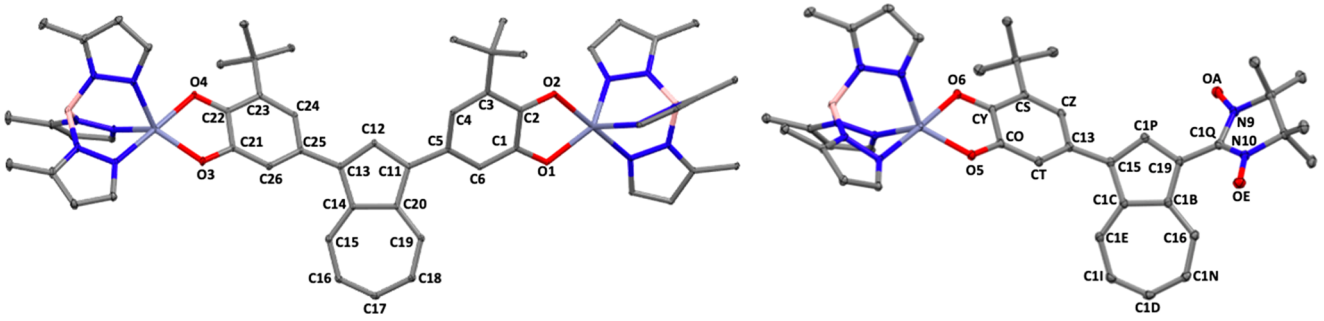

Figure 3. Thermal ellipsoid plots (50% probability) and biradical ligand atomic numbering schemes for X-ray structures of **1,3-SQ$_2$Az** (left) and **1,3-SQ-Az-NN** (right).

(OH) (Tp^{Cum,Me} = hydrotris(3-methyl-5-cumenylpyrazolyl)-borate)[87] and subsequently oxidized with atmospheric O_2 to yield **1,3-SQ$_2$Az**. The [Tp^{Cum,Me}]$^-$ ancillary ligand is a facial tridentate chelating ligand that is both bulky and encapsulating. This property of the ligand effectively insulates the semiquinones from intramolecular interactions in the solid state and has now been used as an ancillary ligand across several dozen semiquinone complexes.[83−85,88−92]

The complex **1,3-SQ-Az-NN** was synthesized as shown in Scheme 1. The synthesis begins with the selective NBS bromination of azulene, which was subsequently coupled with **HOPhBpin** using modified Suzuki conditions to give **HOPh-Az**. Following a substrate-optimized protocol similar to that of Magdziak *et al.*, the phenol was oxidized to the quinone via the regioselective reaction with IBX in DMF then reduced to the catechol with H_2/Pd/C and simultaneously protected with acetate groups due to inherent instability of this free catechol to give **Ac$_2$Cat-Az**. In our hands, the only successful method of installing the NN in the presence of the acetate-protected catechol was to use the known palladium-mediated cross-coupling reaction of **NNAuPPh$_3$** and aryl halides as described by Okada *et al.*[42,93,94] Therefore, the azulene ring of **Ac$_2$Cat-Az** was iodinated selectively with *N*-iodosuccinimide and then cross-coupled with **NNAuPPh$_3$** to give **Ac$_2$Cat-Az-NN**. The final steps to synthesize **1,3-SQ-Az-NN** were performed with modifications to the standard procedure using Tp^{Cum,Me}Zn-(OH) and K_2CO_3 in MeOH/CH_2Cl_2. *In situ* removal of the acetates ensued in basic methanolic solution by slow addition of **Ac$_2$Cat-Az-NN** in CH_2Cl_2 to Tp^{Cum,Me}Zn(OH), and this was followed by complexation with the (Tp^{Cum,Me}Zn)$^+$ complex cation. This procedure was necessary to prevent decomposition of the reactive free catechol-azulene.

https://doi.org/10.1021/acs.joc.1c02085
J. Org. Chem. XXXX, XXX, XXX−XXX

Table 1. Select 1,3-SQ_2Az and 1,3-SQ-Az-NN Bond Lengths[a]

	1,3-SQ_2Az				1,3-SQ-Az-NN	
moiety	bond	length (Å)	bond	length (Å)	bond	length (Å)
SQ C−O	C21−O3	1.296	C1−O1	1.300	CO−O5	1.298
	C22−O4	1.270	C2−O2	1.268	CY−O6	1.266
SQ rings	C21−C22	1.474	C1−C2	1.473	CO−CY	1.473
	C22−C23	1.444	C2−C3	1.446	CY−CS	1.449
	C23−C24	1.369	C3−C4	1.372	CS−CZ	1.365
	C24−C25	1.437	C4−C5	1.431	CZ−C13	1.445
	C25−C26	1.384	C5−C6	1.391	C13−CT	1.389
	C26−C21	1.395	C6−C1	1.400	CT−CO	1.407
SQ−Az bonds	C25−C13	1.463	C5−C11	1.463	C15−C13	1.451
NN bonds					N9−OA	1.288
					N10−OE	1.284
					N9−C1Q	1.371
					N10−C1Q	1.325
Az−NN					C19−C1Q	1.446

[a]See the Supporting Information for crystallographic information.

X-ray Crystallography. X-ray quality crystals of **1,3-SQ_2Az** and **1,3-SQ-Az-NN** were grown by slow evaporation of CH_2Cl_2/MeOH solutions, and the structures determined by X-ray diffraction are shown in Figure 3. The crystal structure shows intermolecular N−O contacts of 3.27 Å suggesting a weak[42] intermolecular antiferromagnetic interaction[95] (see the Supporting Information). The dioxolene C−O and C−C bond lengths for both structures are consistent with the $S = 1/2$ semiquinone anionic spin and charge distribution (see Table 1 for relevant bond lengths).[91] Bond length deviation parameters, $\Sigma|\Delta_i|$,[96,97] defined as the difference in SQ ring bond lengths of 3,5-di-*tert*-butylsemiquinone and those of **1,3-SQ_2Az** and **1,3-SQ-Az-NN**, are 0.154 and 0.153 Å (see the Supporting Information), respectively, possibly indicating a greater delocalization of the SQ spin into the Az bridge than for either **SQ-*m*-Ph-NN** ($\Sigma|\Delta_i| = 0.142$ Å)[91] or **1,3-SQ_2Ph** ($\Sigma|\Delta_i| = 0.129$ Å).[43] Notably, the SQ-Az single bond lengths for both **1,3-SQ_2Az** and **1,3-SQ-Az-NN** are ∼1.46 Å, and this is also consistent with a substantial interaction between the SQ and Az π-systems. The SQ-Az single bond length in **1,3-SQ-Az-NN** is ∼1.45 Å and is therefore slightly shorter that the corresponding bonds in **1,3-SQ_2Az**.

The torsion angle between the SQ ring and azulene bridging unit in **1,3-SQ-Az-NN** is ∼42°, while the torsion angle between the ONCNO π-system of the NN radical and azulene bridging unit is ∼40°. The corresponding torsion angle for **1,3-SQ_2Az** is ∼32°, which is notably less than those of **1,3-SQ-Az-NN**.

Electron Paramagnetic Resonance (EPR) Spectroscopy. Support for a triplet-state of **1,3-SQ_2Az** biradical complex is provided by the frozen-solution EPR spectrum, Figure 4A. The spectral features centered ∼3340 G are consistent with the fine structure of a randomly oriented triplet with a 5% monoradical impurity. Zero-field splitting (ZFS) parameters for the triplet state determined by spectral simulation are $g_{xx} = 2.0040$, $g_{yy} = 2.0032$, $g_{zz} = 2.0054$; $|D/hc| = 0.0040$ cm^{-1}, and $|E/hc| = 0.0004$ cm^{-1}. The formally $\Delta m_s = 2$ transition of the triplet is observed as the characteristic half-field transition (Figure 4A, inset). These ZFS parameters are very close to those of the *m*-Ph-bridged complexes ($D \sim 0.004$ cm^{-1} and $E \sim 0.0001$ cm^{-1}) which is expected due to the fact that in $S > 1/2$ organic species the magnitude of the ZFS is determined by dipole−dipole interactions since the spin−orbit coupling is minimal.[98]

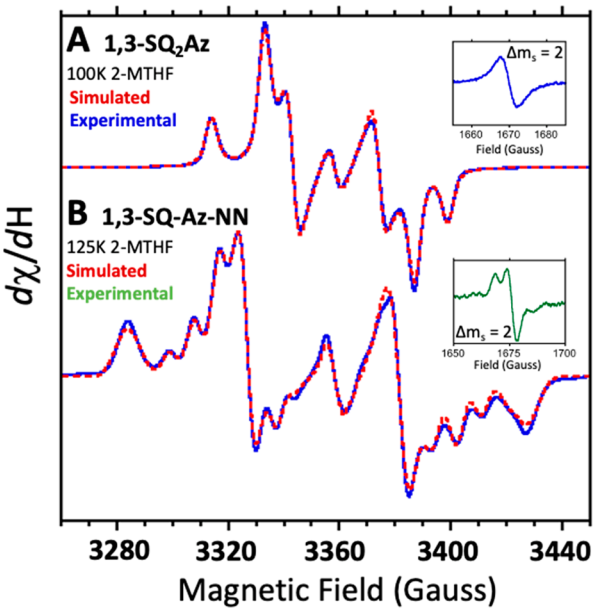

Figure 4. X-band EPR spectra of **1,3-SQ_2Az** (A) and **1,3-SQ-Az-NN** (B) recorded at 100 and 125 K, respectively, in 2-methyltetrahydrofuran (2-MTHF). Simulations were performed using Easyspin.

The frozen solution triplet spectrum of the **1,3-SQ-Az-NN** biradical is presented in Figure 4B. As was observed for **1,3-SQ_2Az**, the spectral features centered ∼3340 G are consistent with the fine structure of a randomly oriented rhombic triplet ($g_{xx} = 2.00606$, $g_{yy} = 2.00277$, $g_{zz} = 2.00518$; $|D/hc| = 0.0067$ cm^{-1}, and $|E/hc| = 0.0004$ cm^{-1}) with a 6% monoradical impurity and an anisotropic ^{14}N hyperfine interaction ($A_{N,xx} = 0.053$ G, $A_{N,yy} = 8.76$ G, $A_{N,zz} = 2.57$ G), similar to the corresponding spectrum of **1,3-NN-Az**.[42,99,100] The formally forbidden $\Delta m_s = 2$ transition of the triplet, which possesses observable ^{14}N hyperfine splitting, is present near half-field (Figure 4B, inset).

The EPR spectral breadth ($= 2D \sim r_e^{-3}$, where r_e is the interelectron separation)[98] of **1,3-SQ_2Az** and **1,3-SQ-Az-NN** differ by a factor of ∼50%, consistent with the shorter SQ−NN spin−spin distance compared to the SQ−SQ spin−spin distance, and consistent with the spectral trends for **1,3-IN_2-Az** and **1,3-NN_2-Az**.[42] However, the room-temperature solution

https://doi.org/10.1021/acs.joc.1c02085
J. Org. Chem. XXXX, XXX, XXX−XXX

EPR spectrum of $S = 1/2$ **1-SQ-Az** (see the Supporting Information) exhibits a ^{1}H-hyperfine pattern that strongly suggests delocalization into both the 5- and 7-membered rings of the azulene π-system, and such delocalization is required for "strong" magnetic exchange with the second radical be it a second SQ (a D-B-D biradical, **1,3-SQ$_2$Az**) or an NN (a D-B-A biradical, **1,3-SQ-Az-NN**).

Electronic Absorption Spectroscopy. The electronic absorption spectra of **1,3-SQ$_2$Az** and **1,3-SQ-Az-NN**, as well as the $S = 1/2$ monoradical-substituted azulenes **1-NN-Az** and **1-SQ-Az**, are shown in Figure 5. The radical **1-NN-Az** has the characteristic NN visible band near 16000 cm^{-1} as well as features between 23000 and 28000 cm^{-1}. While the 27000 cm^{-1} band is characteristic of aryl-substituted NN radicals,[101,102] the lower energy feature is unique to **1-AzNN**. Both **1-SQAz** and **1,3-SQ$_2$Az** possess their own transitions near 27000 cm^{-1}, and they also display an intense (ε_{max} = ~20000−30000 M^{-1}·cm^{-1}), structured transition near 20000 cm^{-1}. Surprisingly, this band *decreases* in intensity when a second SQ group is added (compare the spectra of **1-SQAz** and **1,3-SQ$_2$Az**) and decreases further in **1,3-SQ-Az-NN**. In addition, both **1-SQAz** and **1,3-SQ$_2$Az** possess the characteristic SQ transition[14] in the visible near 12000 cm^{-1}. This 12000 cm^{-1} band in **1-SQAz** is far more intense in (ε_{max} = ~2500 M^{-1}·cm^{-1}) than the corresponding band in **1,3-SQ-Az-NN** (ε_{max} = ~800 M^{-1}·cm^{-1}).

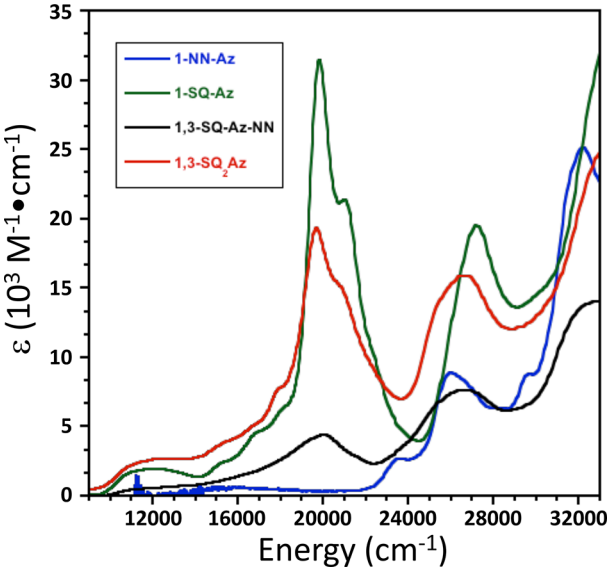

Figure 5. Electronic absorption spectra 300 K/CH_2Cl_2 solvent) of **1,3-SQ$_2$Az** (red line), **1,3-SQ-Az-NN** (black line), and constituent monoradical-substituted azulenes **1-NN-Az** (blue line) and **1-SQ-Az** (green line).

Collectively, the spectra of **1,3-SQ$_2$Az** and **1,3-SQ-Az-NN** illustrate striking differences compared to SQ−bridge−NN D−B−A biradicals with alternant π-system bridges (*e.g.*, *p*-Ph, 2,5-thiophenyl, *etc.*), as well as SQ-bridge-SQ biradicals with cross-conjugated, alternant π-system bridges. D-B-A biradicals with alternant π-system bridges exhibit electronic absorption spectral features of the constituent chromophores plus a characteristic π(SQ) → π^*(bridge−NN) interligand charge transfer transition (Figure 2D) that plays a key role in our VBCI model for donor−bridge−acceptor biradicals (Figure 2D).[14,80,82] Biradicals of the type SQ−bridge−SQ with cross-conjugated, alternant π-system bridges have the spectral features of the SQ−bridge.[44] However, the electronic absorption spectra of **1,3-SQ-Az-NN** and **1,3-SQ-Az-NN** are substantially more complex and exhibit transitions across the entire spectral region. Thus, the use of electronic absorption spectroscopy to elucidate superexchange coupling pathways involving nonalternant bridges will involve the synthesis and spectroscopic study of additional compounds coupled with the results of detailed computational studies.

Magnetic Susceptibility. Variable-temperature magnetic susceptibility measurements were used to determine the sign and magnitude of intramolecular magnetic exchange coupling between the two SQ rings through the nonalternant azulene π-system. Saturation magnetization experiments at 2 K yielded a saturation magnetization (M_{sat}) of 1.7 Bohr magnetons, consistent with a triplet ground state (ferromagnetic coupling of radical spins; see Figure S1). Paramagnetic susceptibility (χ_{para}) data for **1,3-SQ$_2$Az** and **1,3-SQ-Az-NN** were collected between 5 and 300 K in an applied magnetic field of 0.7 T, and these data are shown in Figure 6A,B, respectively. Fitting a simple two-spin singlet−triplet model to the χ_{para}·T vs T data

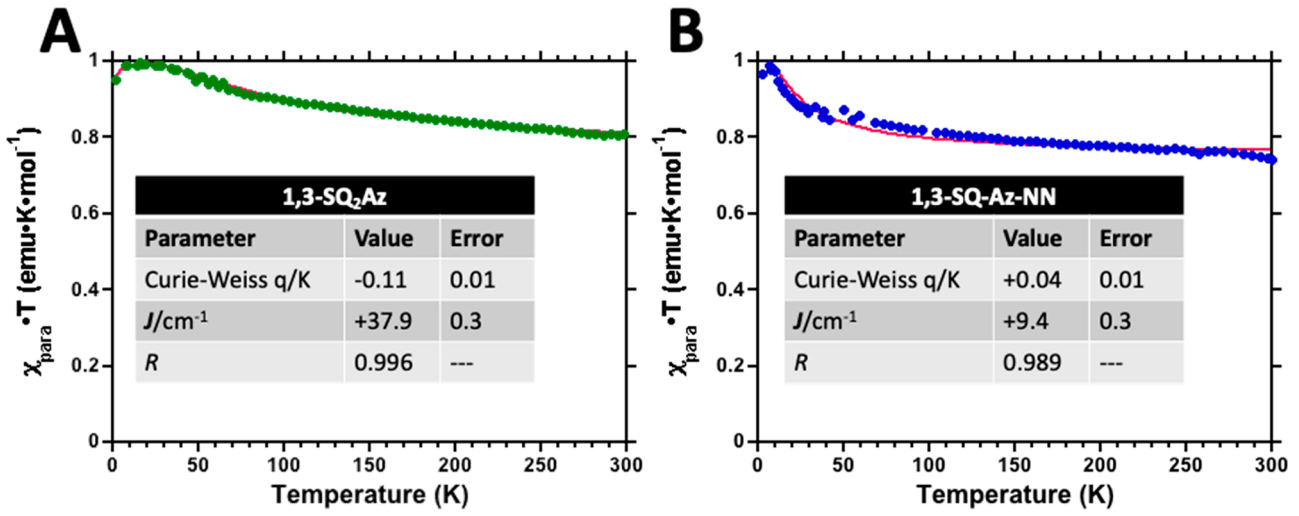

Figure 6. Plots of paramagnetic susceptibility-temperature product (χ_{para}·T) vs temperature for crystalline samples of **1,3-SQ$_2$Az** (A) and **1,3-SQ-Az-NN** (B). Values for fit parameters indicate triplet ground states for both complexes (see text).

https://doi.org/10.1021/acs.joc.1c02085
J. Org. Chem. XXXX, XXX, XXX−XXX

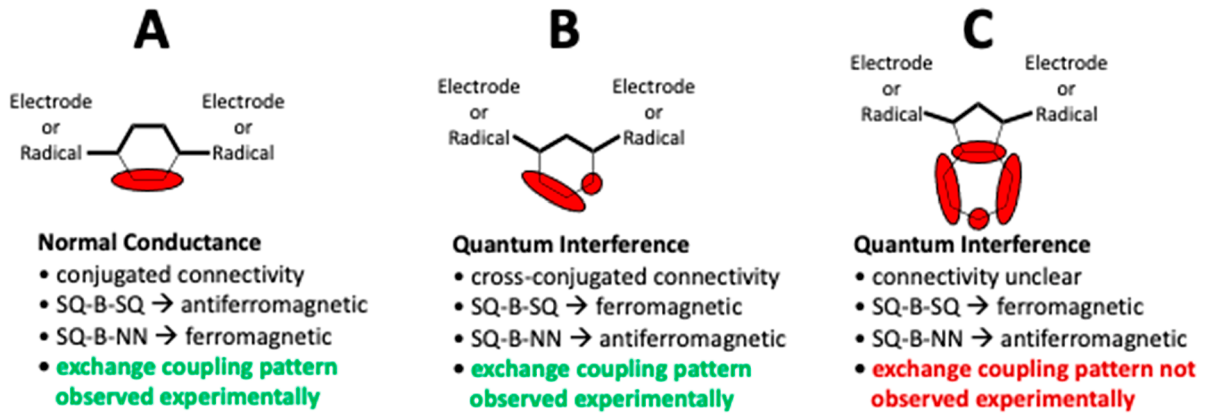

Figure 7. Graphical method for determining normal conductance (via conjugative interaction) or quantum interference (via cross-conjugative interaction) in molecular devices. (A) *p*-Phenylene represents a conjugative pathway between electrodes or radicals. (B) *m*-Phenylene represents a cross-conjugative pathway between electrodes or radicals. (C) Azulene represents the 1,3-pathway through a nonalternant π-system between electrodes or radicals.

resulted in an exchange coupling constant J = +38 cm^{-1} ($\mathcal{H} = -2J\widehat{S_1}\cdot\widehat{S_2}$ exchange Hamiltonian) for **1,3-SQ$_2$Az**, and J = +9 cm^{-1} for **1,3-SQ-Az-NN**. Commensurate with the crystal packing for **1,3-SQ$_2$Az**, a fit to a tetramer (4-spin) model gives $J_{SQ\text{-}NN}$ = +4 cm^{-1} (and J_{inter} = −1.8 cm^{-1}; see the Supporting Information). The positive J values confirm a pairwise ferromagnetic interaction between the two radicals in *both* complexes through the nonalternant bridge giving a triplet ground states. The J value determined for **1,3-SQ$_2$Az** is very similar in both sign and magnitude to those determined previously for **1,3-SQ$_2$Ph-X** with J = +46 cm^{-1} (X = H), J = +36 cm^{-1} (X = OMe), and J = 35 cm^{-1} (X = NMe$_2$).[44] Conversely, the weak ferromagnetic exchange determined for **1,3-SQ-Az-NN** is less than the ferromagnetic coupling observed in **SQ-*p*-Ph-NN** (J = +100 cm^{-1}).[91] The **1,3-SQ-Az-NN** J value is also weaker and of the opposite sign for **SQ-*m*-Ph-NN** (J = −32 cm^{-1}).[76] The larger SQ-bridge and NN-bridge torsion angles for **1,3-SQ$_2$Az** may play a mitigating role in the diminished coupling compared to both phenylene-bridged biradicals.

What is important here is that the magnetic exchange coupling parameter, J, for *both* **1,3-SQ$_2$Az** and **1,3-SQ-Az-NN** is *ferromagnetic*. These results are in striking contrast to the J values for bis-SQ- and SQ-NN biradicals bridged by alternant π-systems: cross conjugated SQ-bridge-SQ biradicals exhibit ferromagnetic exchange, while cross-conjugated SQ-Bridge-NN biradicals exhibit antiferromagnetic exchange.[53,72] Conversely, conjugated SQ-Bridge-SQ species are expected to be either diamagnetic and possess closed-shell Kekulé resonance forms or possess weakly antiferromagnetic exchange, while conjugated SQ-Bridge-NN biradicals exhibit ferromagnetic exchange exchange.[14,76,80,82−85,91] Thus, the observed ferromagnetic coupling in both **1,3-SQ$_2$Az** and **1,3-SQ-Az-NN** is anomalous and further demonstrates the breakdown of orbital-related rules for magnetic exchange coupling in organic biradicals.

Also noteworthy is the *weak* ferromagnetic exchange in **1,3-SQ-Az-NN**, where the exchange coupling parameter in **SQ-*p*-Ph-NN** is +100 cm^{-1}. This is over 10-fold greater than that of **1,3-SQ-Az-NN**.[82,91] The weak exchange in **1,3-SQ-Az-NN** can be attributed, at least in part, to the larger SQ-Az and Az-NN torsion angles compared to the corresponding torsion angles in **SQ-*m*-Ph-NN**.[76] In SQ-Bridge-NN biradicals with alternant, conjugative π-system bridges, the exchange can be understood in terms of a superexchange model (Figure 2D) in which the SQ→Bridge-NN excited charge transfer configuration plays a key role. In azulene bridged systems, the LUMO is nearly nodal at the 1,3 positions,[29] effectively eliminating this superexchange pathway.

Finally, the stated relationships between magnetic exchange coupling and molecular conductance[1,2,20,23] suggests that the graphical method of Markussen[103] might be used to predict exchange coupling through azulene. Figure 7 illustrates this method for predicting quantum interference (typical of cross-conjugated connectivity[22] of electrodes in a molecular junction configuration) or normal conductance via a conjugative interaction pathway for *p*-phenylene (Figure 7A), *m*-phenylene (Figure 7B), and azulene (Figure 7C). The shortest pathway is highlighted with bold bond lines. If the remaining atoms can be grouped together in pairs, then normal conductance is predicted, and is typical for a conjugative pathway (Figure 7A).

Single atoms left unmatched indicate quantum interference behavior (Figures 7B, C). As can be seen, *para*-phenylene (Figure 7A) represents a conjugative pathway which results in normal conductance in single-molecule devices, antiferromagnetic exchange in, *e.g.*, SQ-*p*-Ph-SQ species (closed-shell Kekulé structures), and ferromagnetic coupling in **SQ-*p*-Ph-NN** (observed experimentally[91]). The opposite trends are predicted and observed for cross-conjugated *meta*-phenylene (Figure 7B). The intrinsic conductance through azulene is unclear from break junction experiments,[27,29,104] and so the predictions of this model as they apply to both conductance and magnetic exchange coupling have yet to be resolved. Thus, straightforward models for understanding electronic coupling through azulene, a representative nonalternant π-system, remain elusive.

■ CONCLUSIONS

Herein we described the syntheses, X-ray crystal structures, electron absorption- and EPR spectra, and magnetic exchange properties of two azulene-bridged biradicals **1,3-SQ$_2$Az** and **1,3-SQ-Az-NN**. Both **1,3-SQ$_2$Az** and **1,3-SQ-Az-NN** exhibit ferromagnetic exchange between their constituent radicals, as illustrated by magnetic susceptibility measurements, and the exchange parameters were compared to corresponding biradicals with alternant π-system bridges. To date, there are no straightforward models for predicting magnetic exchange coupling in biradicals with nonalternant π-system bridges.

https://doi.org/10.1021/acs.joc.1c02085
J. Org. Chem. XXXX, XXX, XXX−XXX

Additional synthetic, spectroscopic, and theoretical research is necessary to elucidate coupling pathways through nonalternant π-system bridges and these studies are ongoing in our laboratories.

EXPERIMENTAL SECTION

4-Bromo-2-*tert*-butylphenol[105] and 1,3-dibromoazulene were synthesized according to established literature procedures.[37] **MOM$_2$CatBpin** was prepared according to a modification (see the Supporting Information) of the literature method.[105] 2-Iodoxybenzoic acid (IBX) was prepared by reaction of commercially available 2-iodobenzoic acid and Oxone (potassium peroxymonosulfate) according to the literature procedure.[106] *N*-Bromosuccinimide was recrystallized from water and dried prior to use. *N*-Iodosuccinimide was purchased from Matrix Scientific and used as received. Nitronyl nitroxide-2-ido(triphenylphosphine)gold(I) (NN-Au-PPh$_3$) was prepared according to the literature.[93,94] 2-Isopropoxy-4,4,5,5-tetramethyl-1,3,2-dioxaborolane (*i*-PrOBpin) was purchased from TCI and used as received. 2-*tert*-Butylphenol was purchased from Sigma-Aldrich and used as received.

5-Bromo-3-*tert*-butyl-*o*-quinone (BQ-Br). IBX (29.71 g, 106.1 mmol) was added to a stirred solution of 4-bromo-2-*tert*-butylphenol (18.70 g, 81.62 mmol) in 180 mL of 25% MeOH/CH_2Cl_2 in a room-temperature water bath. Stirred for 20 min, then added 18 g of silica gel and concentrated to dryness under reduced pressure. The solid mixture was loaded onto a column of 224 g of silica gel and purified by flash chromatography using 10% Et_2O/hexanes as eluent. The product-containing fractions were concentrated to give the title compound as a dark solid (17.06 g, 86%) and was used directly in the next step due to instability.

5-Bromo-3-*tert*-butyl-catechol (CatBr). Compound BQ-Br (17.06 g, 70.18 mmol) was dissolved in 90 mL of THF and 90 mL of H_2O, then $Na_2S_2O_4$ (15.88 g, 91.23 mmol) was added and stirred until the solution became light yellow. The reaction mixture was transferred to a separatory funnel, extracted with hexanes and washed with brine. Separated and dried the organic layer with $MgSO_4$, then concentrated under reduced pressure to quantitatively give a yellow oil. No further purification was performed and the yellow oil was used directly in the next step.

5-Bromo-1-*tert*-butyl-2,3-bis(methoxymethoxy)benzene (MOM$_2$CatBr). CatBr from the previous step in 85 mL of CH_2Cl_2 and cooled to 0 °C under nitrogen. (*i*-Pr)$_2$EtN (85 mL, 490 mmol) and DMAP (0.100 g, 0.820 mmol) were added and the reaction was stirred for 10 min. A 1:1 (mol:mol by ^{1}H NMR integration) MOMCl/MeOAc solution ($\delta \approx 0.9$ g/mL, 48 mL, 280 mmol) was added dropwise. A nitrogen-purged condenser was attached, and the reaction was heated to reflux in an oil bath overnight. After the reaction was cooled to room temperature, 100 mL of saturated NH_4Cl solution was added, and the mixture was stirred for 20 min. The mixture was transferred reaction to a separatory funnel, washed with brined and extracted with $CHCl_3$. The organic layer was separated and dried with $MgSO_4$, filtered, and concentrated under reduced pressure. The dark red oil was loaded onto a silica pad and eluted with 20% Et_2O/hexanes and then concentrated to give the title compound as a yellow oil (20.14 g, 86%). ^{1}H NMR (400 MHz, $CDCl_3$) δ: 7.18 (d, J = 2.4 Hz, 1H), 7.10 (d, J = 2.4 Hz, 1H), 5.16 (s, 2H), 5.14 (s, 2H), 3.63 (s, 2H), 3.49 (s, 2H), 1.39 (s, 9H). ^{13}C{^{1}H} NMR (101 MHz, $CDCl_3$) δ: 150.9, 145.3, 145.2, 123.7, 117.9, 115.7, 99.1, 95.5, 57.7, 56.4, 35.4, 30.4. HRMS (ESI-ion trap) m/z: [M + Na]$^+$ Calcd for $C_{14}H_{21}BrO_4Na$ 355.0515; Found 355.0516.

2-(3-*tert*-Butyl-4,5-bis(methoxymethoxy)phenyl)-4,4,5,5-tetramethyl-1,3,2-dioxaborolane (MOM$_2$CatBpin). **MOM$_2$CatBr** (5.96 g, 17.89 mmol) was added to an 250 mL oven-dried round-bottom flask and was purge-pumped; backfilling with nitrogen (3 times). Then *ca.* 125 mL of anhydrous, deoxygenated THF was added, and under nitrogen, the flask was cooled to −78 °C. A solution of *t*-BuLi in hexane (23 mL, 39 mmol) was added dropwise and the reaction was stirred for 10 min at −78 °C after the addition was complete. *i*-PrOBpin (4.4 mL, 22 mmol) was added dropwise, the reaction stirred for 1.5 h at −78 °C, and then the cold bath was removed, and the reaction was allowed to warm to room temperature. Solvent was removed under reduced pressure, and the viscous orange oil was loaded onto a silica pad, eluted with 30% Et_2O/hexanes, and concentrated. The resulting yellow oil was redissolved in minimal pentane and an existing crystalline piece of **MOM$_2$CatBpin** was added and the product was precipitated overnight in a 4 °C refrigerator. The precipitate was washed gently with cold pentane which was pipetted off and then the title compound as a white solid was dried under a stream of nitrogen (6.05 g, 89%). ^{1}H NMR (400 MHz, $CDCl_3$) δ: 7.46 (d, J = 1.3 Hz, 1H), 7.40 (d, J = 1.3 Hz, 1H), 5.23 (s, 2H), 5.21 (s, 2H), 3.65 (s, 3H), 3.52 (s, 3H), 1.44 (s, 9H), 1.32 (s, 12H). ^{13}C{^{1}H} NMR (101 MHz, $CDCl_3$) δ: 149.7, 149.1, 142.9, 127.4, 120.6, 99.2, 95.5, 83.8, 77.4, 57.8, 56.7, 35.2, 30.7, 25.0. HRMS (ESI-ion trap) m/z: [M + Na]$^+$ Calcd for $C_{20}H_{33}BO_6Na$ 403.2262; Found 403.2260.

1,3-Bis(3-*tert*-butyl-4,5-bis(methoxymethoxy)phenyl)-azulene (1,3-(MOM$_2$Cat)$_2$Az). 1,3-Dibromoazulene (112 mg, 0.392 mmol) in 10 mL of argon-purged THF was cannula transferred into a 50 mL round-bottom flask, equipped with magnetic stir bar and a solution of **MOM$_2$CatBpin** (298 mg, 0.784 mmol), Pd(PPh$_3$)$_4$ (9 mg, 8 μmol), and Cs_2CO_3 (516 mg, 1.58 mmol) in 5 mL each of argon-purged THF and H_2O, preheated to 55 °C in an oil bath. A nitrogen-purged reflux condenser was attached and the mixture was stirred at this temperature for 18 h. After cooling to room temperature, the reaction was transferred to a separatory funnel, diluted with Et_2O and washed with brine. The organic layer was separated, dried with $MgSO_4$, and concentrated under reduced pressure. The product was purified by silica gel (deactivated with 1% Et_3N in eluent) chromatography with 10% EtOAc/hexanes to afford 235 mg (96%) of the title compound as a blue oil. ^{1}H NMR (400 MHz, $CDCl_3$) δ: 8.51 (d, J = 9.4 Hz, 2 H), 8.07 (s, 1 H), 7.56 (t, J = 9.8 Hz, 1 H), 7.30 (d, J = 2.3 Hz, 2 H), 7.27 (d, J = 2.3 Hz, 2 H), 7.10 (dd, J = 9.4, 9.8 Hz, 2 H), 5.30 (s, 4 H), 5.25 (s, 4 H), 3.71 (s, 6 H), 3.54 (s, 6 H), 1.50 (s, 18 H). ^{13}C{^{1}H} NMR (400 MHz, $CDCl_3$) δ: 150.2, 144.8, 143.5, 138.9, 137.0, 136.4, 136.2, 132.0, 130.4, 123.2, 122.2, 116.2, 99.1, 95.5, 56.9, 35.3, 30.6. HRMS (APCI$^+$-TOF) m/z: [M + H]$^+$ Calcd for $C_{39}H_{49}O_8$ 633.3427; Found 633.3429.

1,3-SQ$_2$Az. A solution of **1,3-(MOM$_2$Cat)$_2$Az** (75 mg, 0.12 mmol) in 5 mL of MeOH and 0.5 mL of 12 M HCl was stirred for 12 h at room temperature. The mixture was transferred to a separatory funnel, diluted with Et_2O, and washed with brine. The organic layer was separated, dried with Na_2SO_4, and concentrated under reduced pressure. The crude product was carried into the next reaction without further purification, where KOH (14 mg, 0.25 mmol) and Tp^{Cum,Me}Zn-(OH) (164 mg, 0.237 mmol) were combined in a 50 mL round-bottom flask and purge-pumped three times, backfilling with nitrogen. A deoxygenated, anhydrous 1:1 MeOH:CH_2Cl_2 solution (20 mL) was added and the contents were stirred for 1.5 h under nitrogen, then opened and exposed to air for 18 h. The reaction solution was concentrated under reduced pressure leaving *ca.* 5 mL of MeOH. The mixture was then cooled and filtered through a Büchner funnel and the precipitate was washed with cold MeOH and dried to give **1,3-SQ$_2$Az** (69 mg, 32%) of the as a dark green solid. X-ray quality crystals were grown by slow evaporation of a mixture of minimal CH_2Cl_2 in MeOH. IR (solid) ν (cm^{-1}): 2533 (w, B-H). HRMS (APCI$^+$-TOF) m/z: [M + H]$^+$ Calcd for $C_{108}H_{121}B_2N_{12}O_4Zn_2$ 1797.8475; Found 1797.8394.

1-Bromoazulene (Br-Az). To a solution of azulene (154 mg, 1.20 mmol) of in 30 mL of Et_2O at −78 °C was added solid NBS (217 mg, 1.22 mmol). The reaction was stirred for 15 min at −78 °C and then warmed to room temperature and stirred overnight for 16 h. The reaction mixture was transferred to a separatory funnel and washed with 1 M NaOH, then brine. The organic layer was separated, dried with $MgSO_4$, and concentrated under reduced pressure to give 1-bromoazulene (244 mg, 99%) as a dark blue oil, which was used without further purification.

4-(Azulen-1-yl)-2-*tert*-butylphenol (HOPh-Az). A 25 mL round-bottom flask containing **Br-Az** (270 mg, 1.30 mmol), **HOPhBpin** (365 mg, 1.32 mmol), Cs_2CO_3 (850 mg, 2.61mmol), and Pd(PPh$_3$)$_4$ (22 mg, 19 μmol, 1.5 mol %) in 20 mL of THF and 14 mL of H_2O under nitrogen was fitted with a nitrogen-purged, water-cooled condenser and then heated in an oil bath to 55 °C for 20 h. After this time, the reaction mixture was transferred to a separatory funnel,

https://doi.org/10.1021/acs.joc.1c02085
J. Org. Chem. XXXX, XXX, XXX−XXX

diluted with 15 mL of Et_2O, and washed two times each with 10 mL of brine. The organic layer was separated, dried with Na_2SO_4, and concentrated under reduced pressure. The crude material was purified by silica gel flash chromatography with 50% CH_2Cl_2/hexanes to afford 281 mg (78%) of the title compound as a dark blue solid. ^{1}H NMR (400 MHz, $CDCl_3$) δ: 8.51 (d, J = 9.8 Hz, 1 H), 8.33 (d, J = 9.4 Hz, 1 H), 7.99 (d, J = 3.9 Hz, 1 H), 7.57 (dd, J = 9.8, 9.8 Hz, 1 H), 7.53 (d, J = 1.9 Hz, 1 H), 7.43 (d, J = 3.9 Hz, 1 H), 7.33 (dd, J = 1.9, 8.0 Hz, 1 H), 7.12 (dd, J = 9.4, 9.8 Hz, 1 H), 6.82 (d, J = 8.0 Hz, 1 H), 4.79 (s, 1 H), 1.49 (s, 9 H). ^{13}C{^{1}H} NMR (101 MHz, $CDCl_3$) δ: 153.1, 141.4, 138.0, 137.1, 136.3, 135.6, 135.0, 131.7, 129.8, 128.7, 128.6, 128.0, 122.8, 122.6, 117.2, 116.8, 34.7, 29.7. HRMS (ESI-ion trap) m/z: $[M]^+$ Calcd for $C_{20}H_{20}O$ 276.1509; Found 276.1510.

5-(Azulen-1-yl)-3-*tert*-butyl-1,2-phenylene Diacetate (Ac_2Cat-Az). IBX (144 mg, 0.514 mmol) was added to a solution of **HOPh-Az** (126 mg, 0.456 mmol) in 3 mL of DMF. The reaction was stirred for 2 h at room temperature, and then this solution was added dropwise via cannula to a stirring solution of $Pd(OAc)_2$ (101 mg, 0.5 mmol), Cs_2CO_3 (318 mg, 0.976 mmol), and Ac_2O (0.90 mL, 9.5 mmol) in 1 mL of DMF, which had hydrogen bubbled through it for 30 min prior to addition and was under a hydrogen atmosphere. More hydrogen gas was bubbled through the solution. After 1.5 h, TLC (eluting with 100% CH_2Cl_2) confirmed that the reaction was complete. Nitrogen was then bubbled through the solution for 30 min, and the solution was filtered through a pad of Celite and washed with CH_2Cl_2. The filtrate was transferred to a separatory funnel where it was washed with three 50 mL aliquots of water. The organic layer was separated, dried with $MgSO_4$, and concentrated under reduced pressure to afford a crude brown oil. The product was purified by a silica gel column, eluting with 50% CH_2Cl_2/hexanes to afford 94 mg (55%) of the title compound as a blue oil. ^{1}H NMR (400 MHz, $CDCl_3$) δ: 8.58 (d, J = 9.8 Hz, 1 H), 8.37 (d, J = 9.8 Hz, 1 H), 8.01 (d, J = 3.5 Hz, 1 H), 7.62 (dd, J = 9.8, 9.8 Hz, 1 H), 7.51 (d, J = 2.3 Hz, 1 H), 7.44 (d, J = 3.5 Hz, 1 H), 7.35 (d, J = 2.3 Hz, 1 H), 7.21 (d, J = 9.8 Hz, 1 H), 7.17 (d, J = 9.8 Hz, 1 H), 2.40 (s, 3 H), 2.32 (s, 3 H), 1.43 (s, 9 H). ^{13}C{^{1}H} NMR (101 MHz, $CDCl_3$) δ: 168.4, 168.2, 143.0, 142.8, 141.7, 139.4, 138.3, 137.3, 137.0, 135.5, 135.3, 135.2, 130.1, 125.8, 123.6, 123.2, 122.2, 117.4, 35.0, 30.3. HRMS (APCI$^+$-TOF) m/z: $[M + H]^+$ Calcd for $C_{24}H_{25}O_4$ 377.1753; Found 377.1752.

3-*tert*-Butyl-5-(3-iodoazulen-1-yl)-1,2-phenylene Diacetate (Ac_2Cat-Az-I). Ac_2**Cat-Az** (48 mg, 0.17 mmol) was dissolved in *ca.* 30 mL of Et_2O and cooled to −78 °C. *N*-Iodosuccinimide (44 mg, 0.20 mmol) was added, and the mixture was stirred for 20 min at −78 °C, then warmed to room temperature, and stirred for 18 h. The reaction mixture was transferred to a separatory funnel and washed with saturated $NaHCO_3$ solution and then brine, and the organic layer was extracted, dried with $MgSO_4$, and concentrated under reduced pressure to afford Ac_2**Cat-Az-I** (69 mg, 76%) as a dark blue solid. ^{1}H NMR (400 MHz, CD_2Cl_2) δ: 8.48 (d, J = 9.8 Hz, 1 H), 8.30 (d, J = 9.8 Hz, 1 H), 8.08 (s, 1 H), 7.70 (dd, J = 9.8, 9.8 Hz, 1 H), 7.46 (d, J = 2.3 Hz, 1 H), 7.28 (d, J = 2.3 Hz, 1 H), 7.36−7.23 (m, 2 H), 2.37 (s, 3 H), 2.27 (s, 3 H), 1.39 (s, 9 H). ^{13}C{^{1}H} NMR (101 MHz, $CDCl_3$) δ: 168.3, 168.2, 143.3, 142.8, 140.5, 139.8, 139.6, 139.2, 136.4, 135.4, 133.8, 131.4, 128.7, 127.2, 125.7, 124.7, 124.1, 122.2, 74.6, 35.0, 30.3, 20.9, 20.8. HRMS (ESI-ion trap) m/z: $[M + H]^+$ Calcd for $C_{24}H_{23}IO_4$ 503.0714; Found 503.0697.

3-*tert*-Butyl-5-(3-(4,4,5,5,-tetramethyl4,5-dihydroimidazol-3-oxide-1-oxyl)azulen-1-yl)-1,2-phenylene Diacetate (Ac_2Cat-Az-NN). In a 25 mL round-bottom flask, Ac_2**Cat-Az-I** (54 mg, 0.11 mmol), NN-Au-PPh_3 (74 mg, 0.12 mmol), and $Pd(PPh_3)_4$ (13 mg, 0.011 mmol, 10 mol %) were combined under nitrogen. Then 5 mL of THF was added, a nitrogen-purged, water-cooled condenser was attached, and the flask was heated in an oil bath to 60 °C. After 4 h, the reaction was complete as determined by TLC on basic alumina with 33% EtOAc/hexanes, and then it was cooled to room temperature and concentrated under reduced pressure. The title compound was purified by basic alumina column chromatography with 25% EtOAc/hexanes as eluent to afford Ac_2**Cat-Az-NN** (43 mg, 73%) as a dark seafoam green solid. HRMS (APCI$^+$-TOF) m/z: $[M + H]^+$ Calcd for $C_{31}H_{36}N_2O_6$ 532.2573; Found 532.2574.

1,3-SQ-Az-NN. A purge-pumped 50 mL flask containing Ac_2**Cat-Az-NN** (58 mg, 0.11 mmol) in 20 mL of CH_2Cl_2 was added dropwise via cannula at a rate of one drop per 6 seconds to a solution of $Tp^{Cum,Me}Zn(OH)$ (76 mg, 0.11 mmol) and K_2CO_3 (30 mg, 0.22 mmol) in 10 mL of CH_2Cl_2 and 5 mL of MeOH. The green Ac_2**Cat-Az-NN** solution became brown when added to the $Tp^{Cum,Me}Zn(OH)$ and K_2CO_3 solution and then became orange-red. The addition was complete after approximately 3 h, at which point the reaction was opened to air and monitored by EPR. The reaction became red-violet and 77K EPR showed a triplet spectrum. The reaction was stirred open to air for 3 h and then concentrated under reduced pressure to remove the CH_2Cl_2 and the resulting precipitate in MeOH was collected via vacuum filtration. The red-violet solid was collected from the filter paper in a separate flask by dissolving it with Et_2O and then concentrated under reduced pressure to afford **1,3-SQ-Az-NN** (71 mg, 58%) as a red-violet solid. HRMS (ESI-TOF) m/z: $[M + H]^+$ Calcd for $C_{66}H_{75}BN_8O_4Zn$ 1117.5332; Found 1117.5276. X-ray quality crystals were grown from CH_2Cl_2/*i*-PrOH layer−layer diffusion.

1-SQAz. A purge-pumped 50 mL flask containing Ac_2**Cat-Az** (65 mg, 0.17 mmol) in 31 mL of CH_2Cl_2 was added dropwise via cannula at a rate of one drop per 2 seconds to a solution of $Tp^{Cum,Me}Zn(OH)$ (114 mg, 0.16 mmol) and K_2CO_3 (48 mg, 0.35 mmol) in 16 mL of CH_2Cl_2 and 8 mL of MeOH. The green Ac_2**Cat-Az** solution became brown when added to the $Tp^{Cum,Me}Zn(OH)$ and K_2CO_3 solution and then became orange-red. The addition was complete after approximately 3.5 h at which point the reaction was opened to air and monitored by EPR. The reaction became red-violet. The reaction was stirred open to air overnight and then concentrated under reduced pressure to remove the CH_2Cl_2, and the resulting precipitate in MeOH was collected via vacuum filtration. The red-violet solid was collected from the filter paper in a separate flask by dissolving it with Et_2O and then concentrated under reduced pressure to afford **SQ-Az** (104 mg, 68%) as a red-violet solid. HRMS (ESI-TOF) m/z: $[M + H]^+$ Calcd for $C_{59}H_{65}BN_6O_2Zn$ 964.4563; Found 964.4520.

1-NNAz. In a 25 mL round-bottom flask, 1-iodoazulene (40 mg, 0.16 mmol), NN-Au-PPh_3 (96 mg, 0.16 mmol), and $Pd(PPh_3)_4$ (18 mg, 0.016 mmol, 10 mol %) were combined to under nitrogen. Then 5 mL of THF was added, a nitrogen-purged, water-cooled condenser was attached, and the flask was heated in an oil bath to 55 °C. After 6 h, the reaction was complete as determined by TLC on basic alumina with 50% CH_2Cl_2/hexanes; the mixture was was cooled to room temperature and then concentrated under reduced pressure. The title compound was purified by basic alumina column chromatography with 50% CH_2Cl_2/hexanes as eluent to afford **1-NNAz** (22 mg, 50%) as a dark seafoam green solid. HRMS (ESI-TOF) m/z: $[M + 2H]^+$ Calcd for $C_{17}H_{21}N_2O_2$ 285.1603; Found 285.1609.

■ ASSOCIATED CONTENT

Supporting Information

The Supporting Information is available free of charge at https://pubs.acs.org/doi/10.1021/acs.joc.1c02085.

X-ray crystallographic information, magnetization plots, NMR spectra, HRMS spectra, and fluid solution EPR spectrum of **1-SQAz** (PDF)

Accession Codes

CCDC 2106044−2106045 contain the supplementary crystallographic data for this paper. These data can be obtained free of charge via www.ccdc.cam.ac.uk/data_request/cif, or by emailing data_request@ccdc.cam.ac.uk, or by contacting The Cambridge Crystallographic Data Centre, 12 Union Road, Cambridge CB2 1EZ, UK; fax: +44 1223 336033.

■ AUTHOR INFORMATION

Corresponding Authors

David A. Shultz − *Department of Chemistry, North Carolina State University, Raleigh, North Carolina 27695-8204, United*

https://doi.org/10.1021/acs.joc.1c02085
J. Org. Chem. XXXX, XXX, XXX−XXX

States; orcid.org/0000-0001-8121-6812; Email: shultz@ncsu.edu

Martin L. Kirk − *Department of Chemistry, The University of New Mexico, Albuquerque, New Mexico 87131-0001, United States;* orcid.org/0000-0002-1479-3318; Email: mkirk@unm.edu

Author

Patrick Hewitt − *Department of Chemistry, North Carolina State University, Raleigh, North Carolina 27695-8204, United States*

Complete contact information is available at: https://pubs.acs.org/10.1021/acs.joc.1c02085

Author Contributions

The manuscript was written through contributions of all authors.

Notes

The authors declare no competing financial interest.

■ ACKNOWLEDGMENTS

D.A.S. acknowledges financial support from NSF (CHE-1931291 and CHE-1764181). M.L.K. acknowledges financial support from NSF (CHE-1900237). This work was performed in part by the Molecular Education, Technology and Research Innovation Center (METRIC) at NC State University, which is supported by the State of North Carolina. Mass spectra were obtained either at the NCSU Mass Spectrometry Facility which is part of METRIC at NC State University or at the Michigan State University Mass Spectrometry and Metabolomics Core facility. Funding for D8 VENTURE acquisition was provided in part by North Carolina Biotechnology Center grant: NCBC#2019-IDG-1010.

■ REFERENCES

(1) Herrmann, C. Electronic Communication as a Transferable Property of Molecular Bridges? *J. Phys. Chem. A* **2019**, *123*, 10205−10223.

(2) Kirk, M. L.; Dangi, R.; Habel-Rodriguez, D.; Yang, J.; Shultz, D. A.; Zhang, J. Transferrable Property Relationships Between Magnetic Exchange Coupling and Molecular Conductance. *Chem. Sci.* **2020**, *11*, 11425−11434.

(3) Nitzan, A. A Relationship between Electron-Transfer Rates and Molecular Conduction. *J. Phys. Chem. A* **2001**, *105*, 2677−2679.

(4) Ratner, M. A brief history of molecular electronics. *Nat. Nanotechnol.* **2013**, *8*, 378−381.

(5) Solomon, G. C.; Bergfield, J. P.; Stafford, C. A.; Ratner, M. A. When "small" terms matter: Coupled interference features in the transport properties of cross-conjugated molecules. *Beilstein J. Nanotechnol.* **2011**, *2*, 862−871.

(6) Bergfield, J. P.; Solomon, G. C.; Stafford, C. A.; Ratner, M. A. Novel Quantum Interference Effects in Transport through Molecular Radicals. *Nano Lett.* **2011**, *11*, 2759−2764.

(7) Ricks, A. B.; Solomon, G. C.; Colvin, M. T.; Scott, A. M.; Chen, K.; Ratner, M. A.; Wasielewski, M. R. Controlling Electron Transfer in Donor-Bridge-Acceptor Molecules Using Cross-Conjugated Bridges. *J. Am. Chem. Soc.* **2010**, *132* (43), 15427−15434.

(8) Herrmann, C.; Solomon, G. C.; Ratner, M. A. Organic Radicals As Spin Filters. *J. Am. Chem. Soc.* **2010**, *132* (11), 3682−3684.

(9) Hansen, T.; Solomon, G. C.; Andrews, D. Q.; Ratner, M. A. Interfering pathways in benzene: An analytical treatment. *J. Chem. Phys.* **2009**, *131*, 194704.

(10) Chernick, E. T.; Mi, Q.; Vega, A. M.; Lockard, J. V.; Ratner, M. A.; Wasielewski, M. R. Controlling Electron Transfer Dynamics in Donor - Bridge - Acceptor Molecules by Increasing Unpaired Spin Density on the Bridge. *J. Phys. Chem. B* **2007**, *111*, 6728−6737.

(11) Shu, C.; Pink, M.; Junghoefer, T.; Nadler, E.; Rajca, S.; Casu, M. B.; Rajca, A. Synthesis and Thin Films of Thermally Robust Quartet (S = 3/2) Ground State Triradical. *J. Am. Chem. Soc.* **2021**, *143* (14), 5508−5518.

(12) Junghoefer, T.; Gallagher, N. M.; Kolanji, K.; Giangrisostomi, E.; Ovsyannikov, R.; Chasse, T.; Baumgarten, M.; Rajca, A.; Calzolari, A.; Casu, M. B. Challenges in Controlled Thermal Deposition of Organic Diradicals. *Chem. Mater.* **2021**, *33* (6), 2019−2028.

(13) Calzolari, A.; Rajca, A.; Casu, M. B. From radical to triradical thin film processes: the Blatter radical derivatives. *J. Mater. Chem. C* **2021**, *9*, 10787−10793.

(14) Shultz, D. A.; Kirk, M. L.; Zhang, J.; Stasiw, D. E.; Wang, G.; Yang, J.; Habel-Rodriguez, D.; Stein, B. W.; Sommer, R. D. Spectroscopic Signatures of Resonance Inhibition Reveal Differences in Donor-Bridge and Bridge-Acceptor Couplings. *J. Am. Chem. Soc.* **2020**, *142*, 4916−4924.

(15) Mahendran, A.; Gopinath, P.; Breslow, R. Single molecule conductance of aromatic, nonaromatic, and partially antiaromatic systems. *Tetrahedron Lett.* **2015**, *56* (33), 4833−4835.

(16) Chen, W. B.; Li, H. X.; Widawsky, J. R.; Appayee, C.; Venkataraman, L.; Breslow, R. Aromaticity Decreases Single-Molecule Junction Conductance. *J. Am. Chem. Soc.* **2014**, *136* (3), 918−920.

(17) Breslow, R.; Foss, F. W. Charge transport in nanoscale aromatic and antiaromatic systems. *J. Phys.: Condens. Matter* **2008**, *20* (37), 374104.

(18) Rajca, A. The physical organic chemistry of very high-spin polyradicals. In *Adv. Phys. Org. Chem.*; Richard, J. P., Ed.; Elsevier, 2005; Vol. *40*, pp 153−199.

(19) Cardamone, D. M.; Stafford, C. A.; Mazumdar, S. Controlling quantum transport through a single molecule. *Nano Lett.* **2006**, *6* (11), 2422−2426.

(20) Tsuji, Y.; Hoffmann, R.; Strange, M.; Solomon, G. C. Close relation between quantum interference in molecular conductance and diradical existence. *Proc. Natl. Acad. Sci. U. S. A.* **2016**, *113*, E413−E419.

(21) Borges, A.; Solomon, G. C. Effects of Aromaticity and Connectivity on the Conductance of Five-Membered Rings. *J. Phys. Chem. C* **2017**, *121* (15), 8272−8279.

(22) Valkenier, H.; Guédon, C. M.; Markussen, T.; Thygesen, K. S.; van der Molen, S. J.; Hummelen, J. C. Cross-conjugation and quantum interference: a general correlation? *Phys. Chem. Chem. Phys.* **2014**, *16*, 653−662.

(23) Kirk, M. L.; Shultz, D. A.; Zhang, J.; Dangi, R.; Ingersol, L.; Yang, J.; Finney, N. S.; Sommer, R. D.; Wojtas, L. Heterospin Biradicals Provide Insight into Molecular Conductance and Rectification. *Chem. Sci.* **2017**, *8*, 5408−5415.

(24) Ueda, A.; Nishida, S.; Fukui, K.; Ise, T.; Shiomi, D.; Sato, K.; Takui, T.; Nakasuji, K.; Morita, Y. Three-Dimensional Intramolecular Exchange Interaction in a Curved and Nonalternant pi-Conjugated System: Corannulene with Two Phenoxyl Radicals. *Angew. Chem., Int. Ed.* **2010**, *49* (9), 1678−1682.

(25) Noll, G.; Avola, M.; Lynch, M.; Daub, J. Comparison of alternant and nonalternant aromatic bridge systems with respect to their ET-properties. *J. Phys. Chem. C* **2007**, *111* (7), 3197−3204.

(26) Noll, G.; Amthor, S.; Avola, M.; Lambert, C.; Daub, J. Charge resonance excitations in 1,3-bis di(4-methoxyphenyl)aminolazulene radical cations. *J. Phys. Chem. C* **2007**, *111* (8), 3512−3516.

(27) Xia, J.; Capozzi, B.; Wei, S.; Strange, M.; Batra, A.; Moreno, J. R.; Amir, R. J.; Amir, E.; Solomon, G. C.; Venkataraman, L.; Campos, L. M. Breakdown of Interference Rules in Azulene, a Nonalternant Hydrocarbon. *Nano Lett.* **2014**, *14*, 2941−2945.

(28) Strange, M.; Solomon, G. C.; Venkataraman, L.; Campos, L. M. Reply to "Comment on 'Breakdown of Interference Rules in Azulene, a Nonalternant Hydrocarbon'. *Nano Lett.* **2015**, *15* (11), 7177−7178.

(29) Schwarz, F.; Koch, M.; Kastlunger, G.; Berke, H.; Stadler, R.; Venkatesan, K.; Lörtscher, E. Charge Transport and Conductance Switching of Redox-Active Azulene Derivatives. *Angew. Chem., Int. Ed.* **2016**, *55* (39), 11781−11786.

(30) Beer, M.; Longuet-Higgins, H. C. Anomalous Light Emission of Azulene. *J. Chem. Phys.* **1955**, *23* (8), 1390−1391.
(31) Viswanath, G.; Kasha, M. Confirmation of the Anomalous Fluorescence of Azulene. *J. Chem. Phys.* **1956**, *24* (3), 574−577.
(32) Bearpark, M. J.; Bernardi, F.; Clifford, S.; Olivucci, M.; Robb, M. A.; Smith, B. R.; Vreven, T. The azulene S-1 state decays *via* a conical intersection: A CASSCF study with MMVB dynamics. *J. Am. Chem. Soc.* **1996**, *118* (1), 169−175.
(33) Wurzer, A. J.; Wilhelm, T.; Piel, J.; Riedle, E. Comprehensive measurement of the S-1 azulene relaxation dynamics and observation of vibrational wavepacket motion. *Chem. Phys. Lett.* **1999**, *299* (3−4), 296−302.
(34) Schwarzer, D.; Troe, J.; Votsmeier, M.; Zerezke, M. Collisional deactivation of vibrationally highly excited azulene in compressed liquids and supercritical fluids. *J. Chem. Phys.* **1996**, *105* (8), 3121−3131.
(35) Liu, R. S. H. Colorful azulene and its equally colorful derivatives. *J. Chem. Educ.* **2002**, *79* (2), 183−185.
(36) Schwarz, F.; Koch, M.; Kastlunger, G.; Berke, H.; Stadler, R.; Venkatesan, K.; Lortscher, E. Charge Transport and Conductance Switching of Redox-Active Azulene Derivatives. *Angew. Chem., Int. Ed.* **2016**, *55* (39), 11781−11786.
(37) Koch, M.; Blacque, O.; Venkatesan, K. Impact of 2,6-connectivity in azulene: optical properties and stimuli responsive behavior. *J. Mater. Chem. C* **2013**, *1* (44), 7400−7408.
(38) Yamaguchi, Y.; Takubo, M.; Ogawa, K.; Nakayama, K.; Koganezawa, T.; Katagiri, H. Terazulene Isomers: Polarity Change of OFETs through Molecular Orbital Distribution Contrast. *J. Am. Chem. Soc.* **2016**, *138* (35), 11335−11343.
(39) Eberson, L.; GonzalezLuque, R.; Merchan, M.; Radner, F.; Roos, B. O.; Shaik, S. Radical cations of non-alternant systems as probes of the Shaik-Pross VB configuration mixing model. *J. Chem. Soc., Perkin Trans. 2* **1997**, No. 3, 463−472.
(40) Lambert, C.; Noll, G.; Zabel, M.; Hampel, F.; Schmalzlin, E.; Brauchle, C.; Meerholz, K. Highly substituted azulene dyes as multifunctional NLO and electron-transfer compounds. *Chem. - Eur. J.* **2003**, *9* (17), 4232−4239.
(41) Launay, J. P. An orbital approach of electron transfer in multisite systems. Implications for carbon-rich spacers. *Polyhedron* **2015**, *86*, 151−166.
(42) Haraguchi, M.; Tretyakov, E.; Gritsan, N.; Romanenko, G.; Gorbunov, D.; Bogomyakov, A.; Maryunina, K.; Suzuki, S.; Kozaki, M.; Shiomi, D.; Sato, K.; Takui, T.; Nishihara, S.; Inoue, K.; Okada, K. (Azulene-1,3-diyl)-bis(nitronyl nitroxide) and (Azulene-1,3-diyl)-bis-(iminonitroxide) and Their Copper Complexes. *Chem. - Asian J.* **2017**, *12* (22), 2929−2941.
(43) Sloop, J. C.; Shultz, D. A.; Coote, T.; Shepler, B.; Sullivan, U.; Kampf, J. W.; Boyle, P. D. Synthesis of and structure-property relationships in zinc complexes of bis-metaphenylene semiquinone biradical species. *J. Phys. Org. Chem.* **2012**, *25*, 314−321.
(44) Shultz, D. A.; Bodnar, S. H.; Lee, H.; Kampf, J. W.; Incarvito, C. D.; Rheingold, A. L. The Singlet-Triplet Gap in Triplet Ground-State Biradicals Is Modulated by Substituent Effects. *J. Am. Chem. Soc.* **2002**, *124*, 10054−10061.
(45) Kahn, O. *Molecular Magnetism*; VCH: New York, 1993.
(46) Kirk, M. L.; Shultz, D. A.; Depperman, E. C. Beyond the active-electron approximation: Origin of ferromagnetic exchange in donor-acceptor heterospin biradicals. *Polyhedron* **2005**, *24*, 2880−2884.
(47) Borden, W. T.; Davidson, E. R. Effects of Electron Repulsion in Conjugated Hydrocarbon Diradicals. *J. Am. Chem. Soc.* **1977**, *99*, 4587−4594.
(48) Borden, W. T.; Iwamura, H.; Berson, J. A. Violations of Hund's Rule in Non-Kekulé Hydrocarbons: Theoretical Prediction and Experimental Verification. *Acc. Chem. Res.* **1994**, *27*, 109−116.
(49) Borden, W. T. *Diradicals*; Wiley: New York, 1982.
(50) Salem, L.; Rowland, C. The Electronic Properties of Diradicals. *Angew. Chem., Int. Ed. Engl.* **1972**, *11*, 92.
(51) Tretyakov, E. V.; Zhivetyeva, S. I.; Petunin, P. V.; Gorbunov, D. E.; Gritsan, N. P.; Bagryanskaya, I. Y.; Bogomyakov, A. S.; Postnikov, P. S.; Kazantsev, M. S.; Trusova, M. E.; Shundrina, I. K.; Zaytseva, E. V.; Parkhomenko, D. A.; Bagryanskaya, E. G.; Ovcharenko, V. I. Ferromagnetically Coupled S = 1 Chains in Crystals of Verdazyl-Nitronyl Nitroxide Diradicals. *Angew. Chem., Int. Ed.* **2020**, *59* (46), 20704−20710.
(52) Petunin, P. V.; Rybalova, T. V.; Trusova, M. E.; Uvarov, M. N.; Kazantsev, M. S.; Mostovich, E. A.; Postulka, L.; Eibisch, P.; Wolf, B.; Lang, M.; Postnikov, P. S.; Baumgarten, M. A Weakly Antiferromagnetically Coupled Biradical Combining Verdazyl with Nitronylnitroxide Units. *ChemPlusChem* **2020**, *85* (1), 159−162.
(53) Baumgarten, M., High Spin Organic Molecules. In *World Scientific Reference on Spin in Organics*; Miller, J. S., Ed.; World Scientific Publishing: Singapore, 2018; Vol. *IV*, pp 1−93.
(54) Ovchinnikov, A. A. Multiplicity of the Ground State of Large Alternant Organic Molecules with Conjugated Bonds (Do Organic Ferromagnetics Exist?). *Theoret. Chim. Acta (Berl.)* **1978**, *47*, 297.
(55) Misurkin, I. A.; Ovchinnikov, A. A. The Electronic Structures and Properties of Polymeric Molecules with Conjugated Bonds. *Russ. Chem. Rev.* **1977**, *46*, 967.
(56) Longuet-Higgins, H. C. Some Studies in Molecular Orbital Theory I. Resonance structures and Molecular Orbitals in Unsaturated Hydrocarbons. *J. Chem. Phys.* **1950**, *18*, 265.
(57) Kollmar, H.; Staemmler, V. Violation of Hund's Rule by Spin Polarization in Molecules. *Theoret. Chim. Acta (Berl.)* **1978**, *48*, 223−239.
(58) Karafiloglou, P. Through bond interaction of two radical centers: Analysis of the spin polarization and related mechanisms in linear π diradicals. *J. Chem. Phys.* **1985**, *82*, 3728−3740.
(59) Salem, L. *Molecular Orbital Theory of Conjugated Systems*; W. A. Benjamin, Inc.: New York, 1966.
(60) Salem, L. Intermolecular Orbital Theory of Interaction Between Conjugated Systems. 1. General Theory Cycloadditions. *J. Am. Chem. Soc.* **1968**, *90*, 543.
(61) Vostrikova, K. E. High-spin molecules based on metal complexes of organic free radicals. *Coord. Chem. Rev.* **2008**, *252*, 1409−1419.
(62) Caneschi, A.; Dei, A.; Lee, H.; Shultz, D. A.; Sorace, L. A Ferromagnetically Coupled Bis-Semiquinone Ligand Enforces High-Spin Ground States in Bis-Metal Complexes. *Inorg. Chem.* **2001**, *40*, 408−411.
(63) Miller, J. S. Organic magnets - A history. *Adv. Mater.* **2002**, *14* (16), 1105−1110.
(64) Wan, X. J.; Lv, X.; He, G. R.; Yu, A.; Chen, Y. S. Synthesis of neutral stable polyradicals and their application on photovoltaic devices. *Eur. Polym. J.* **2011**, *47* (5), 1018−1030.
(65) Murata, H.; Takahashi, M.; Namba, K.; Takahashi, N.; Nishide, H. A high-spin and durable polyradical: Poly(4-diphenylaminium-1,2-phenylenevinylene). *J. Org. Chem.* **2004**, *69* (3), 631−638.
(66) Caneschi, A.; Dei, A.; Mussari, C. P.; Shultz, D. A.; Sorace, L.; Vostrikova, K. E. High-Spin Metal Complexes Containing a Ferromagnetically-Coupled Tris(Semiquinone) Ligand. *Inorg. Chem.* **2002**, *41*, 1086−1092.
(67) Miyasaka, M.; Yamazaki, T.; Nishide, H. Regioregular Polythiophene with Pendant Phenoxyl Radicals: A New High-Spin Organic Polymer. *Macromolecules* **2000**, *33* (22), 8211.
(68) Sato, O.; Tao, J.; Zhang, Y. Z. Control of magnetic properties through external stimuli. *Angew. Chem., Int. Ed.* **2007**, *46* (13), 2152−2187.
(69) Rajca, A. Organic Diradicals and Polyradicals: From Spin Coupling to Magnetism? *Chem. Rev.* **1994**, *94*, 871−893.
(70) Gallagher, N. M.; Olankitwanit, A.; Rajca, A. High-Spin Organic Molecules. *J. Org. Chem.* **2015**, *80* (3), 1291−1298.
(71) Rajca, A.; Utamapanya, S. Toward Organic Synthesis of a Magnetic Particle: Dendritic Polyradicals with 15 and 31 Centers for Unpaired Electrons. *J. Am. Chem. Soc.* **1993**, *115*, 10688−10694.
(72) Rajca, A. Organic diradicals and polyradicals - from spin coupling to magnetism. *Chem. Rev.* **1994**, *94*, 871.
(73) Rajca, A., High-Spin Polyradicals. In *Magnetic Properties of Organic Materials*; Lahti, P., Ed.; Marcel Dekker, Inc.: New York, 1999; pp 345−359.

https://doi.org/10.1021/acs.joc.1c02085
J. Org. Chem. XXXX, XXX, XXX−XXX

(74) Rajca, A.; Wongsriratanakul, J.; Rajca, S. Magnetic ordering in an organic polymer. *Science* **2001**, *294*, 1503−1505.
(75) Rajca, A. From High-Spin Organic Molecules to Organic Polymers with Magnetic Ordering. *Chem. - Eur. J.* **2002**, *8* (21), 4834−4841.
(76) Kirk, M. L.; Shultz, D. A.; Stasiw, D. E.; Habel-Rodriguez, D.; Stein, B.; Boyle, P. D. Electronic and Exchange Coupling in a Cross-Conjugated D-B-A Biradical: Mechanistic Implications for Quantum Interference Effects. *J. Am. Chem. Soc.* **2013**, *135*, 14713−14725.
(77) Lahti, P. M.; Ichimura, A. S. Semiempirical Study of Electron Exchange Interaction in Organic High-Spin Pi-Systems - Classifying Structural Effects in Organic Magnetic Molecules. *J. Org. Chem.* **1991**, *56* (9), 3030−3042.
(78) Field, L. M.; Lahti, P. M. Coordination complexes of 1-(4- N-tert-butyl-N-aminoxyl phenyl)-1H-1,2,4-triazole with paramagnetic transition metal dications. *Inorg. Chem.* **2003**, *42* (23), 7447−7454.
(79) Borden, W. T.; Davidson, E. R. Theoretical Studies of Diradicals Containing Four Pi Electrons. *Acc. Chem. Res.* **1981**, *14*, 69−76.
(80) Kirk, M. L.; Shultz, D. A.; Depperman, E. C.; Habel-Rodriguez, D.; Schmidt, R. D. Spectroscopic Studies of Bridge Contributions to Electronic Coupling in a Donor-Bridge-Acceptor Biradical System. *J. Am. Chem. Soc.* **2012**, *134*, 7812−7819.
(81) Kirk, M. L.; Shultz, D. A.; Habel-Rodriguez, D.; Schmidt, R. D.; Sullivan, U. Hyperfine Interaction, Spin Polarization, and Spin Delocalization as Probes of Donor-Bridge-Acceptor Interactions in Exchange-Coupled Biradicals. *J. Phys. Chem. B* **2010**, *114*, 14712−14716.
(82) Kirk, M. L.; Shultz, D. A.; Depperman, E. C.; Brannen, C. L. Donor-acceptor biradicals as ground state analogues of photoinduced charge separated states. *J. Am. Chem. Soc.* **2007**, *129*, 1937−1943.
(83) Kirk, M. L.; Shultz, D. A. Transition Metal Complexes of Donor-Acceptor Biradicals. *Coord. Chem. Rev.* **2013**, *257*, 218−233.
(84) Kirk, M. L.; Shultz, D. A.; Stasiw, D. E.; Lewis, G. F.; Wang, G.; Brannen, C. L.; Sommer, R. D.; Boyle, P. D. Superexchange Contributions to Distance Dependence of Electron Transfer/Transport: Exchange- and Electronic Coupling in Oligo(para-Phenylene)- and Oligo(2,5-Thiophene)-Bridged Donor-Bridge-Acceptor Biradical Complexes. *J. Am. Chem. Soc.* **2013**, *135*, 17144−17154.
(85) Stasiw, D. E.; Zhang, J.; Wang, G.; Dangi, R.; Stein, B. W.; Shultz, D. A.; Kirk, M. L.; Wojtas, L.; Sommer, R. D. Determining the Conformational Landscape of σ and π Coupling Using para-Phenylene and "Aviram−Ratner" Bridges. *J. Am. Chem. Soc.* **2015**, *137*, 9222−9225.
(86) Herrmann, C. Electronic Communication as a Transferable Property of Molecular Bridges? *J. Phys. Chem. A* **2019**, *123*, 10205−10223.
(87) Ruf, M.; Vahrenkamp, H. Small Molecule Chemistry of the Pyrazolylborate—Zinc Unit $Tp^{Cum,\ Me}Zn$. *Inorg. Chem.* **1996**, *35*, 6571−6578.
(88) Ruf, M.; Noll, B. C.; Groner, M. D.; Yee, G. T.; Pierpont, C. G. Pocket Semiquinonate Complexes of Cobalt(II), Copper(II, and Zinc(II) Prepared with the Hydrdotris(cumenylmethylpyrazolyl)-borate Ligand. *Inorg. Chem.* **1997**, *36*, 4860−4865.
(89) Sloop, J. C.; Shultz, D. A.; Coote, T.; Shepler, B.; Sullivan, U.; W, K. J.; Boyle, P. D. Synthesis of and Structure-Property Relationships in Zinc Complexes of Bis-Metaphenylene Semiquinone Biradical Species. *J. Phys. Org. Chem.* **2012**, *24* (4), 314−321.
(90) Shultz, D. A.; Mussari, C. P.; Ramanathan, K. K.; Kampf, J. W. Electron spin-spin exchange coupling mediated by the porphyrin pi system. *Inorg. Chem.* **2006**, *45* (15), 5752−5759.
(91) Shultz, D. A.; Vostrikova, K. E.; Bodnar, S. H.; Koo, H.-J.; Whangbo, M.-H.; Kirk, M. L.; Depperman, E. C.; Kampf, J. W. Trends in Metal-Biradical Exchange Interaction for First-Row MII(Nitronyl Nitroxide-Semiquinone) Complexes. *J. Am. Chem. Soc.* **2003**, *125*, 1607−1617.
(92) Shultz, D. A.; Fico, R. M., Jr.; Bodnar, S. H.; Kumar, R. K.; Vostrikova, K. E.; Kampf, J. W.; Boyle, P. D. Trends in Exchange Coupling for Trimethylenemethane-Type Bis(Semiquinone) Biradicals and Correlation of Magnetic Exchange with Mixed Valency for Cross-Conjugated Systems. *J. Am. Chem. Soc.* **2003**, *125*, 11761.
(93) Suzuki, S.; Kira, S.; Kozaki, M.; Yamamura, M.; Hasegawa, T.; Nabeshima, T.; Okada, K. An efficient synthetic method for organometallic radicals: structures and properties of gold(I)-(nitronyl nitroxide)-2-ide complexes. *Dalton Trans.* **2017**, *46* (8), 2653−2659.
(94) Tanimoto, R.; Suzuki, S.; Kozaki, M.; Okada, K. Nitronyl Nitroxide as a Coupling Partner: Pd-Mediated Cross-coupling of (Nitronyl nitroxide-2-ido(triphenylphosphine)gold(I) with Aryl Halides. *Chem. Lett.* **2014**, *43*, 678−680.
(95) Novoa, J. J.; Deumal, M., The mechanism of the through-space magnetic interactions in purely organic molecular magnets. In *π-Electron Magnetism from Molecules to Magnetic Materials*; Veciana, J., Ed.; Springer, 2001; Vol. *100*, pp 33−60.
(96) Shultz, D. A.; Bodnar, S. H.; Kumar, R. K.; Kampf, J. W. Both an Oxidation/Reduction Sequence and Deprotonation of a Unique Paramagnetic Ligand Lead to a Mixed-Valent Complex. *J. Am. Chem. Soc.* **1999**, *121*, 10664−10665.
(97) Shultz, D. A.; Bodnar, S. H.; Kampf, J. W. Molecular Structure of and Exchange Coupling in a Bis(Semiquinone) Complex. *Chem. Commun.* **2001**, 93−94.
(98) Atherton, N. M. *Principles of Electron Spin Resonance*. Ellis Horwood PTR Prentice Hall: New York, 1993.
(99) D'Anna, J. A.; Wharton, J. H. Electron Spin Resonance Spectra of a-Nitronylnitroxide Radicals; Solvent Effect; Nitrogen Hyperfine Tensor; g Anisotropy. *J. Chem. Phys.* **1970**, *53*, 4047.
(100) Jürgens, O.; Vidal-Gancedo, J.; Rovira, C.; Wurst, K.; Sporer, C.; Bildstein, B.; Schottenberger, H.; Jaitner, P.; Veciana, J. Transmission of Magnetic Interactions through an Organometallic Coupler: A Novel Family of Metallocene-Substituted alpha-Nitronyl Aminoxyl Radicals. *Inorg. Chem.* **1998**, *37*, 4547.
(101) Putz, A. M.; Schatzschneider, U.; Rentschler, E. Integrated experimental and computational spectroscopy study on the protonation of the alpha-nitronyl nitroxide radical unit. *Phys. Chem. Chem. Phys.* **2012**, *14* (5), 1649−1653.
(102) Osiecki, J. H.; Ullman, E. F. Studies of free radicals. I. alpha.-Nitronyl nitroxides, a new class of stable radicals. *J. Am. Chem. Soc.* **1968**, *90*, 1078−1079.
(103) Markussen, T.; Stadler, R.; Thygesen, K. S. The Relation between Structure and Quantum Interference in Single Molecule Junctions. *Nano Lett.* **2010**, *10* (10), 4260−4265.
(104) Stadler, R. Comment on "Breakdown of Interference Rules in Azulene, a Nonalternant Hydrocarbon. *Nano Lett.* **2015**, *15* (11), 7175−7176.
(105) Shultz, D. A.; Hollomon, M. G. Preparation and EPR Spectroscopic Investigation of Conjugated Oligomers Containing Semiquinone Repeat Units. *Chem. Mater.* **2000**, *12*, 580−585.
(106) Frigerio, M.; Santagostino, M.; Sputore, S. A user-friendly entry to 2-iodoxybenzoic acid (IBX). *J. Org. Chem.* **1999**, *64*, 4537−4538.

https://doi.org/10.1021/acs.joc.1c02085
J. Org. Chem. XXXX, XXX, XXX−XXX